

## Engineering the Substrate Specificity of D-Amino-acid Oxidase\*

Received for publication, April 23, 2002, and in revised form, May 7, 2002  
Published, JBC Papers in Press, May 20, 2002, DOI 10.1074/jbc.M203946200

Silvia Sacchi, Simona Lorenzi, Gianluca Molla, Mirella S. Pilone, Carlo Rossetti,  
and Loredano Pollegioni‡

From the Department of Structural and Functional Biology, University of Insubria, via J. H. Dunant 3,  
21100 Varese, Italy

The high resolution crystal structure of D-amino-acid oxidase (DAAO) from the yeast *Rhodotorula gracilis* provided us with the tool to engineer the substrate specificity of this flavo-oxidase. DAAO catalyzes the oxidative deamination of D-amino acids, with the exception of D-aspartate and D-glutamate (which are oxidized by D-aspartate oxidase, DASPO). Following sequence homology, molecular modeling, and simulated annealing docking analyses, the active site residue Met-213 was mutated to arginine. The mutant enzyme showed properties close to those of DASPO (e.g. the oxidation of D-aspartate and the binding of L-tartrate), and it was still active on D-alanine. The presence of an additional guanidinium group in the active site of the DAAO mutant allowed the binding (and thus the oxidation) of D-aspartate, but it was also responsible for a lower catalytic activity on D-alanine. Similar results were also obtained when two additional arginines were simultaneously introduced in the active site of DAAO (M213R/Y238R mutant, yielding an architecture of the active site more similar to that obtained for the DASPO model), but the double mutant showed very low stability in solution. The decrease in maximal activity observed with these DAAO mutants could be due to alterations in the precise orbital alignment required for efficient catalysis, although even the change in the redox properties (more evident in the DAAO-benzoate complex) could play a role. The rational design approach was successful in producing an enzymatic activity with a new, broader substrate specificity, and this approach could also be used to develop DAAO variants suitable for use in biotechnological applications.

DAAO; they are substrates of D-aspartate oxidase (EC 1.4.3.1, DASPO). DAAO from the yeast *Rhodotorula gracilis* (RgDAAO) possesses peculiar properties, such as highly efficient catalysis and tight binding with the coenzyme FAD, properties which distinguish it from the mammalian enzyme (2, 4–6), and has many biotechnological applications (3). The crystal structure of RgDAAO, in complex with various substrates/ligands, has recently been determined at a very high resolution (up to 1.2 Å) (7). At the same time, we substantiated the role of the active site residues by site-directed mutagenesis (8–10); analogous to that reported for pig kidney DAAO (11, 12), these residues (namely Tyr-223, Tyr-238, and Arg-285) do not act as an active site base, but they are involved in the correct orientation of the bound substrate with respect to the N(5)-flavin position. According to these results RgDAAO can be considered a paradigm of the importance of orbital steering for efficient catalysis (7), in agreement with Koshland's proposal (see Ref. 13).

Beef kidney DASPO and pig kidney DAAO show a high degree of similarity in terms of molecular weight, primary sequence, and interaction between FAD and the flavin-binding site (14), as well as in the ability to act on D-proline and thiazolidine-2-carboxylic acid (15). Despite these similarities, the kinetic mechanism (the main difference concerns the step where the product is released) (16, 17) and the substrate specificity of the two oxidases differ. The mammalian DAAO and DASPO differ from the yeast DAAO in that the kinetic efficiency is lower (mainly due to a different location of the rate-limiting step) (6, 16, 17).

Industrially, the DAAO reaction has mainly been used to remove the side chain of cephalosporin C to give 7-aminocephalosporanic acid, a key intermediate for the production of semi-synthetic cephalosporin antibiotics (18). The redox reaction of DAAO can also be exploited in the production of  $\alpha$ -keto acids, in the resolution of racemic mixtures of amino acids, and in the analytical determination of D-amino acids (3). D-Isomers of amino acids, formed during food processing as well as originating from microbial sources, are considered indicators of food quality (for a review see Ref. 19) and may become part of the human diet. As a means of quickly and selectively detecting and determining D-amino acid content, an amperometric and a colorimetric biosensor have been devised recently (20) using RgDAAO. However, because the enzyme does not oxidize acidic D-amino acids, it cannot be used to detect the total amount of D-amino acids in biological samples.

We attempted to use rational design as a strategy for understanding the modulation of the substrate specificity exerted by the active site residues of RgDAAO, to obtain an enzyme that is increasingly more suitable for biotechnological applications. In the present study we investigated the features of substrate recognition by DAAO, combining the structural and functional information available on DAAO and DASPO with the simulated annealing docking of D-aspartate at the active site of

D-Amino-acid oxidase (EC 1.4.3.3, DAAO)<sup>1</sup> is considered the paradigm of the dehydrogenase-oxidase class of flavoproteins (1). It catalyzes dehydrogenation of the D-isomer of the amino acids to give the corresponding  $\alpha$ -imino acids and, after subsequent hydrolysis,  $\alpha$ -keto acids and ammonia (for a review see Refs. 2 and 3). DAAO shows a broad substrate specificity; the best substrates are apolar D-amino acids, but it is also active on polar and basic D-amino acids. The acidic D-amino acids glutamate and aspartate are the only D-amino acids not oxidized by

\* This work was supported by Grant PRIN MM05C73482 from Italian Ministero dell'Istruzione, dell'Università e della Ricerca (to M. S. P.). The costs of publication of this article were defrayed in part by the payment of page charges. This article must therefore be hereby marked "advertisement" in accordance with 18 U.S.C. Section 1734 solely to indicate this fact.

‡ To whom correspondence should be addressed. Tel.: 0332-421506; Fax: 0332-421500; E-mail: loredano.pollegioni@uninsubria.it.

<sup>1</sup> The abbreviations used are: DAAO, D-amino-acid oxidase; RgDAAO, *R. gracilis* D-amino-acid oxidase; DASPO, D-aspartate oxidase;  $EF_{ox}^1$ , oxidized enzyme;  $EF_{seq}^1$ , enzyme flavin semiquinone;  $EF_{red}^1$ , reduced enzyme.

DAAO and at the active site of a model of DASPO. We thus report on the rational design and the characterization of a single point mutant (M213R) and of a double mutant (M213R/Y238R) of RgDAAO with a broader substrate specificity, and thus active on both neutral and acidic D-amino acids.

#### EXPERIMENTAL PROCEDURES

**Site-directed Mutagenesis and Enzyme Expression**—Enzymatic DNA modifications were carried out according to the manufacturer's instructions and essentially as described in Sambrook *et al.* (21). The M213R mutant was generated by site-directed mutagenesis (Altered Sites® II kit, Promega), using the cDNA coding for the wild-type RgDAAO subcloned into the pAlter™ vector (8, 9). The mutation was introduced using the following 31-mer mutagenic oligonucleotide GCAAGCGATG-CACGCGTGACTCGTCCGACCC. The mutant cDNA (confirmed by automated DNA sequencing) was subcloned into the *EcoRI* restriction site of the pT7.7A expression vector (pT7-M213R). The double mutant was generated using the cDNA coding for M213R and Y238R single-point mutants. pT7-M213R and pT7-Y238R vectors were digested with *NdeI* and *SexAI*. The two *NdeI*-*SexAI*-digested fragments containing the M213R and the Y238R mutation (of 702 and 2967 bp, respectively) were ligated to give the pT7-M213R/Y238R expression plasmid. The introduction of the desired mutations was confirmed by automated DNA sequencing.

**Activity Assay and Kinetic Measurements**—DAAO activity was assayed with an oxygen electrode at pH 8.5 and 25 °C, using 28 mM D-alanine as substrate (4). One DAAO unit was defined as the amount of enzyme that converted 1 μmol of D-alanine per min at 25 °C. The kinetic parameters of the DAAO reaction with different D-amino acids were determined in 100 mM sodium pyrophosphate buffer, pH 8.5, at 25 °C (22).

**Spectral Experiments, Redox Potentials, and Ligand Binding**—The spectral experiments were carried out in 50 mM HEPES, pH 7.5, 10% glycerol, 5 mM 2-mercaptoethanol, and 0.3 mM EDTA at 15 °C. The extinction coefficient for the oxidized M213R mutant DAAO was determined by measuring the change in absorbance after release of the flavin by heat denaturation (an extinction coefficient of 11,300 M<sup>-1</sup> cm<sup>-1</sup> at 450 nm for free FAD was used). Photoreduction experiments were carried out at 15 °C using an anaerobic cuvette containing 8 μM enzyme, in the buffer described above which contained 5 mM EDTA and 0.5 μM 5-deazaflavin and was made anaerobic by alternative cycles of vacuum and O<sub>2</sub>-free argon (8, 23). The thermodynamic stability of the semiquinone was determined by adding 5 μM benzyl viologen from a side arm of the cuvette after photoreduction had completed. Redox potentials of the M213R mutant were determined by the method of dye equilibration (24) using the xanthine/xanthine oxidase reduction system (25) at 15 °C and in the absence of EDTA and 2-mercaptoethanol. The reaction was initiated by the addition of 10 nM xanthine oxidase to an anaerobic cuvette containing ~10 μM enzyme, 0.2 mM xanthine, 5 μM benzyl viologen, and 1.5–10 μM of the appropriate dye (25, 26). The amount of oxidized and reduced dye and of oxidized, semiquinone, and reduced enzyme was determined spectrophotometrically either at an isosbestic point for the dye or by subtraction of the dye contribution in the 400–500 nm region (26). The redox potential,  $E_h$ , for the system at equilibrium was calculated from the Nernst Equation 1,

$$E_h = E_m + (2.3RT/nF)\log(\text{oxidized form}/\text{reduced form}) \quad (\text{Eq. 1})$$

where  $R$  is the gas constant;  $T$  is the absolute temperature;  $F$  is Faraday's constant; and  $n$  is the number of electrochemical equivalents. The data were then plotted as described by Minnaert (24), *i.e.* the  $\log(\text{oxidized}/\text{reduced})$  couples for the enzyme was plotted against  $\log(\text{oxidized}/\text{reduced})$  concentration ratio for the dye. The  $E_m$  value for the enzyme (two-electron transfer) was determined from the  $\Delta E_m$  value between the standard dye and DAAO from the value of  $\log(\text{oxidized}/\text{reduced})$  for the enzyme when the  $\log(\text{oxidized}/\text{reduced})$  for the dye is zero. The oxidation/reduction potential for one-electron transfer for the couple  $EF_{\text{ox}}^1/EF_{\text{red}}^1$  ( $E_1$ ) was determined by plotting the ratio of the concentrations of the oxidized and semiquinone forms of DAAO, and the one-electron transfer potential for the couple  $EF_{\text{ox}}^1/EF_{\text{red}}^1$  ( $E_2$ ) was similarly determined by plotting the ratio of the concentration of the semiquinone and reduced forms of the enzyme. The separation between the two single-electron transfers was also estimated from the maximal percentage of the semiquinone form of the enzyme reached during a reduction experiment in the absence of the reference dye (25, 26) (Equations 2 and 3).

$$\Delta E_m = 59\text{mV} \times \log K \quad (\text{Eq. 2})$$

$$K = [EF_{\text{seq}}^1]^2/[EF_{\text{red}}^1][EF_{\text{ox}}^1] \quad (\text{Eq. 3})$$

Dissociation constants for ligands were measured spectrophotometrically by addition of small volumes of concentrated stock solutions to samples containing 1 ml of ~10 μM enzyme, at 15 °C. The change in absorbance was plotted as a function of ligand concentration, after correcting for any volume change.

**Amperometric Procedures**—The possibility to use DAAO mutants in a biosensor (Midaspro, Sartorius A.G.) for the detection of D-amino acid concentration was evaluated by means of amperometry in stirred solutions essentially as described previously (20). Small volumes (25–200 μl) of concentrated D-amino acid solution were added to 5 ml of 100 mM sodium pyrophosphate buffer, pH 8.5, in the cell, while stirring at a constant rate and applying a fixed voltage (+400 mV *versus* Ag/AgCl). The steady-state anodic currents were recorded ~3 min after a fixed amount of enzyme had been added in the measuring cell (the time required to reach 95% of the steady-state anodic current). Previously, it was demonstrated for wild-type DAAO that the slope of the current intensity increase, as well as the final value reached, depends on the D-amino acid concentration (20).

**Structure Coordinates of RgDAAO**—In complex with trifluoro-D-alanine, the Protein Data Bank code is 1c0p (7); in complex with anthranilate the Protein Data Bank accession code is 1c0i.

#### RESULTS

**Mutant Design**—The active site of RgDAAO in a complex with trifluoro-D-alanine showed that the α-carboxylic group of the D-amino acid interacts electrostatically with the γ- and ε-amino groups of Arg-285 (at ~2.8 Å), and it was H-bound to the hydroxyl groups of Tyr-223 and Tyr-238. The substrate α-amino group was H-bound symmetrically to the backbone C=O group of Ser-335 and to an active site water molecule, whereas the substrate side chain was oriented toward the hydrophobic binding pocket of the active site (see Fig. 1A) (7). The substrate-binding pocket was encompassed by the side chains of Asn-54, Thr-56, Phe-58, Met-213, Tyr-223, Ile-225, Tyr-238, Arg-285, and Ser-335 (all of these residues are at a distance ≤6 Å from the β-carbon of the D-amino acid). In particular the side chain of Met-213 was 3.8 Å from the β-C group of trifluoro-D-alanine.

By using the Swiss model software at the ExpASy facility (27), a model of the three-dimensional structure of DASPO was predicted, using the protein sequence of DASPO from bovine kidney (27 and 40% amino acid sequence identity with RgDAAO and pig kidney DAAO, respectively) (28, 29) and the crystal structure of DAAO (7, 11). A comparison of the active site of DAAO with the model derived for DASPO showed the presence of two additional arginines in the active site of the latter, which are not present in RgDAAO (Fig. 1B); Arg-216 and Arg-237 seemed to be located in a position resembling that of Met-213 and Tyr-238 in DAAO. D-Aspartate binding into the active site of both RgDAAO and DASPO model was achieved using a Monte Carlo-simulated annealing algorithm that predicted the bound conformations of flexible ligands to macromolecules (AutoDock 2.4 software) (30, 31). Among the theoretical DAAO-D-aspartate complexes, the one possessing the lowest energy conformation contained the substrate in a reverse configuration with respect to that observed with trifluoro-D-alanine, *i.e.* the acidic group of the side chain was located in the position normally occupied by the α-carboxylic group of the substrate (Fig. 2A). This alteration of the orientation of the αC-H bond with respect to the N(5)-flavin position may explain the inactivity of wild-type DAAO toward acidic D-amino acids. In the DASPO model the carboxylic side chain group was involved in a network of electrostatic and hydrogen bonding with neighboring amino acids (in particular with Arg-216 and Arg-237, see Fig. 1B) that correspond to the shell residues with neutral or slightly polar characteristics in DAAO. Therefore, in an effort to stabilize the binding of D-aspartate in the correct orientation at the active site of RgDAAO, the Met-213 residue was mutated in arginine. A theoretical model of the simulated

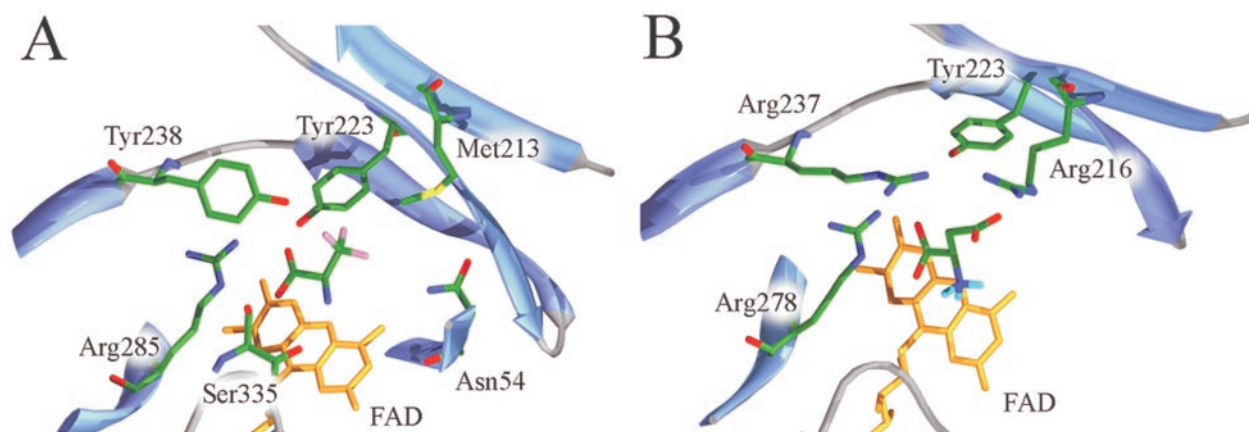


FIG. 1. A, active site of wild-type RgDAAO in complex with trifluoro-D-alanine. The side chain of Met-213 is  $\sim 3.8$  Å from the  $\beta$ -carbon of the bound ligand/substrate. B, proposed model of the active site of wild-type DASPO in complex with D-aspartate. The model has been generated by the Swiss model server (27) using the protein sequence of bovine kidney DASPO (29) and DAAO atomic coordinates (7). Three arginine residues are present at a distance  $\leq 6$  Å from the  $\beta$ -carbon of the substrate/ligand (and Arg-216 seems to be located in a position resembling that of Met-213 in DAAO). Docking of D-aspartate at the active site of DASPO model was achieved as reported above.

docking of D-aspartate at the active site of the mutant is depicted in Fig. 2B. It clearly shows an electrostatic interaction of the carboxylic side chain of D-aspartate with the positively charged side chain of Arg-213 (distance  $\leq 3.3$  Å). With the same aim, an additional arginine was introduced by replacing Tyr-238 in DAAO active site, a position corresponding to Arg-237 in DASPO model (double-point mutant M213R/Y238R DAAO, see Fig. 2C).

**Purification and Properties of M213R DAAO**—The M213R mutant was expressed in *Escherichia coli* and purified using the protocol reported for the wild-type RgDAAO (32). Starting from a 10-liter fermentation broth, 12 mg of pure enzyme with a specific activity of 3.5 units/mg protein was achieved (compared with a figure of 180 mg of pure enzyme with a specific activity of 110 units/mg protein obtained for the recombinant wild-type DAAO) (32). The lower expression of the mutant was not due to protein instability or proteolytic processes, because no proteolysis products have been detected on Western blot of crude extracts. In addition, comparison by Western blot analysis of the amount of DAAO present in the whole cell paste and in the crude extracts excluded inclusion bodies formation. An overall purification yield of  $\geq 30\%$  was obtained. The protein was about 95% pure and yielded a single band at  $\sim 40$  kDa in SDS-PAGE. Like the wild-type enzyme, the purified variant DAAO was a dimeric holoenzyme and was stable when stored at  $-20$  °C for several months. The visible spectrum of the oxidized form of the mutant enzyme showed a hyperchromic change of the flavin peaks (Table I), indicative of a more polar microenvironment surrounding the flavin coenzyme. Anaerobic addition of an excess of D-alanine resulted in the instantaneous and full reduction of the mutant enzyme during mixing (data not shown) (4), demonstrating that the M213R mutant of RgDAAO was competent in catalysis. The specific activity on D-alanine as substrate was significantly reduced in the mutant (Table I). Under anaerobic conditions, the M213R mutant forms an anionic (red) flavin semiquinone on photoreduction (23). Both wild-type and M213R DAAO undergo quite complete semiquinone formation on light irradiation in the presence of EDTA (Table I).

**Kinetics and Binding Properties of M213R DAAO**—To investigate the substrate specificity of M213R DAAO mutant, air-saturated solutions of different substrates were tested by measuring oxygen consumption using a Rank electrode (4) in both wild-type and M213R DAAOs. We reported previously (22) that RgDAAO does not oxidize acidic D-amino acids (no oxygen consumption was detected under standard conditions). The

recent observation (7) that the oxidized enzyme is converted to the corresponding reduced form reacting with D-lactate under anaerobic conditions prompted us to investigate this reaction more thoroughly. Under similar experimental conditions, even D-aspartate and D-glutamate reduced the flavin coenzyme of wild-type RgDAAO (data not shown). Although the polarographic assay did not show a measurable  $O_2$  consumption under standard conditions when an acidic D-amino acid was used as substrate, a detectable trace could be observed by using a large amount ( $\sim 30$ – $80$   $\mu\text{g}$ ) of pure wild-type DAAO and a very high concentration of acidic D-amino acids. On the other hand, the recombinant M213R DAAO showed a detectable trace using the polarographic assay on D-alanine, D-aspartate, and D-glutamate as substrates in the presence of the same low amount of enzyme in the polarographic assay (2–6  $\mu\text{g}$ ). A comparison of the kinetic parameters of M213R DAAO, determined at a fixed (0.253 mM)  $O_2$  concentration using various D-amino acids, with the values determined for wild-type DAAO and with those reported for beef DASPO is shown in Table II. The catalytic efficiency (expressed as  $k_{\text{cat}}/K_m$  ratio) of the M213R DAAO variant on D-aspartate and D-glutamate as substrate was similar to that determined for beef kidney DASPO (and an  $\sim 7$ -fold higher  $k_{\text{cat}}$  value with D-glutamate is also obtained) (33). The appearance of appreciable activity on acidic D-amino acids in the DAAO mutant did not abolish the activity on neutral and polar D-amino acids. The comparison of the substrate specificity profile of wild-type and M213R did not allow us to determine whether Met-213 was involved in the substrate chain length selection process (although a significant increase in the  $K_m$  for D-alanine and D-proline was evident, see Table II).

Measuring the dissociation constant for several ligands also substantiated the contribution of residue at the position occupied by Met-213 in wild-type DAAO to substrate recognition and binding. Binding was measured by following the perturbation of the visible spectrum of the FAD upon formation of the enzyme-ligand complex. The spectral changes on benzoate and anthranilate binding to the M213R DAAO were qualitatively similar to those reported for the wild-type enzyme (4, 22), but smaller changes in absorbance intensity on binding were observed with all the ligands tested, e.g. from the difference spectra of the titration with benzoate, a  $\Delta\epsilon_{497\text{nm}}$  of  $3.2 \text{ mM}^{-1} \text{ cm}^{-1}$  was estimated for the mutant versus  $4.0 \text{ mM}^{-1} \text{ cm}^{-1}$  observed for the wild-type RgDAAO. The introduction of the positively charged guanidinium group of Arg-213 in the mutant

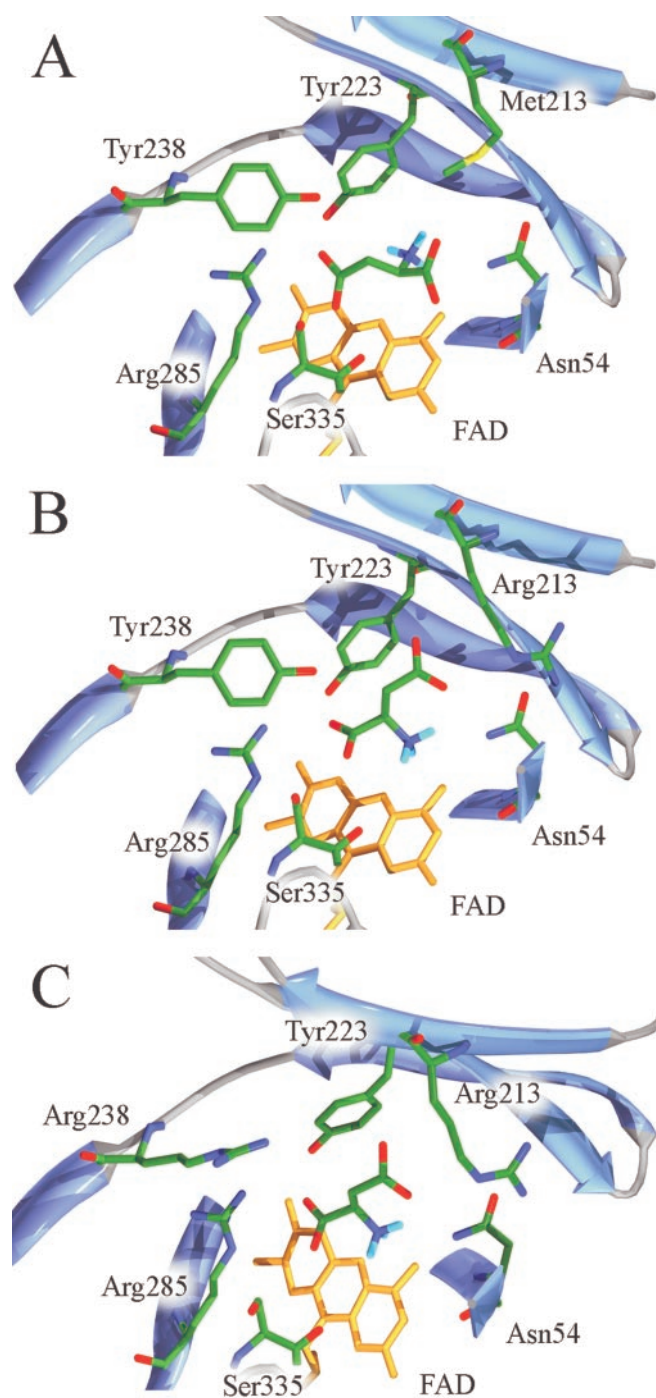


FIG. 2. Proposed models of the active site of wild-type (A), M213R (B), and M213R/Y238R (C) mutants of RgDAAO in complex with D-aspartate. A, the model is the result of a simulated annealing docking of D-aspartate to RgDAAO using the program AutoDock 2.4. It combines a rapid, grid-based method for evaluation of the ligand-protein interaction energies and with a Monte Carlo simulated annealing search algorithm for optimal conformations of ligands (30, 31). B and C, models of M213R and M213R/Y238R DAAO mutants were developed using Swiss PDB viewer program; the docking of the D-aspartate at the active site was achieved as reported above.

not only maintained the binding properties of DAAO (although a small decrease in the binding of large, aromatic carboxylic acids such as benzoate and anthranilate was observed, see Table I), but the ability to bind L(+)-tartrate (Fig. 3), a classical competitive inhibitor of DASPO (14), also evolved. The  $K_d$  value determined with the mutant DAAO ( $K_d = 0.04$  mM) was very close to the value previously determined for beef kidney

TABLE I  
Comparison of properties of wild-type and M213R mutant of *R. gracilis* D-amino-acid oxidase

Experimental conditions are as follows: 50 mM HEPES buffer, pH 7.5, 10% glycerol, 5 mM 2-mercaptoethanol, and 0.3 mM EDTA. Activity was assayed with an oxygen electrode on D-alanine, at pH 8.5 and 25°C (4, 22).

	Wild-type	M213R
General properties		
Aggregation state	Dimeric <sup>a</sup>	Dimeric
Specific activity (units/mg)	110 <sup>a</sup>	3.5
Flavin properties		
$\epsilon_{455\text{nm}}$ oxidized form ( $\text{mM}^{-1} \text{cm}^{-1}$ )	12.6 <sup>a</sup>	13.5
$A_{274}/A_{455}$ ratio	8.2	9.7
Semiquinone measured (%)	$\geq 95^b$	97
$\text{p}K_a\text{N}(3\text{H})$	$10.6 \pm 0.2^c$	$10.6 \pm 0.1$
Binding properties <sup>d</sup>		
$K_d$ for benzoate (mM)	0.9 <sup>b</sup>	6.3
$K_d$ for anthranilate (mM)	1.9 <sup>e</sup>	7.5
$K_d$ for crotonate (mM)	0.8	0.1
$K_d$ for oxalacetate (mM)	1.5	12
$K_d$ for L(+)-tartrate (mM)	No binding	0.04
$K_d$ for sulfite (mM)	0.12 <sup>b</sup>	0.05

<sup>a</sup> From Ref. 32.

<sup>b</sup> From Ref. 4.

<sup>c</sup> From Ref. 38.

<sup>d</sup> Wavelengths used for  $K_d$  determinations were 458 nm for L(+)-tartrate and for sodium sulfite, 482 nm for sodium benzoate and oxalacetate, and 544 nm for sodium anthranilate.

<sup>e</sup> From Ref. 22.

DASPO ( $K_d = 0.03$  mM). Interestingly, the addition of a large amount of carboxylic acids,  $\sim 10$ -fold above the corresponding estimated  $K_d$  value, resulted in spectral changes that resembled those of the FAD dissociation. In fact, gel filtration chromatography on a Sephadex G-25 column of this sample resulted in the resolution of the M213R DAAO apoprotein from the flavin cofactor. Such a behavior was never observed for either the wild-type or all the mutant DAAOs tested (8, 9, 22).

**Redox Properties of M213R**—To assess changes in the thermodynamic properties of the flavin center caused by mutation, and that could be associated to the lower activity of the M213R mutant, the redox potentials were measured using the dye equilibration method (24). The positioning of an arginine at location 213, *i.e.* a second positive charge into the active site of DAAO, resulted in a slight change of the  $K_d$  value for sulfite binding (see Table I). When the xanthine oxidase-mediated reduction of M213R mutant was monitored in the absence of a reference dye, a large amount/percentage of semiquinone was formed during the reduction (85 *versus* 95% for the wild-type enzyme). From the semiquinone stability constant (25) and by using Equations 2 and 3, the separation between the potentials was estimated at  $\sim 125$  mV. The potentials of the oxidized/semiquinone and semiquinone/reduced couples for the free M213R DAAO form have been determined using the dye equilibration method and the dyes listed in Table III (24–26). The redox potential difference with respect to the dye can be calculated plotting the log (oxidized/reduced) of the dye as a function of log (oxidized/semiquinone) or log (semiquinone/reduced) of the enzyme (34). In the absence of ligands, the M213R mutant had a midpoint redox potential  $E_m$  (34) similar to that determined for the wild-type ( $E_1$  and  $E_2$  values for M213R and wild-type RgDAAO are reported in Table III). Analogously to the measurements on the free form, the M213R DAAO-benzoate complex was also reduced using the xanthine/xanthine oxidase system in the presence of benzyl viologen as one-electron mediator. The spectrum of the oxidized enzyme was converted into the semiquinone form (maximal amount of  $\sim 60\%$ ) to yield the reduced form, *i.e.* the one-electron transfer was still the most favored process. On the other hand, for the wild-type

TABLE II

Comparison of the apparent steady-state parameters on various D-amino acids (indicated using the three-letter abbreviations) obtained for wild-type, M213R, and M213R/Y238R (values in parentheses) mutants of *R. gracilis* D-amino-acid oxidases and bovine D-aspartate oxidase

All measurements were performed at 25 °C, in 100 mM sodium pyrophosphate buffer, pH 8.5, at air saturation ( $[O_2] = 0.253$  mM), using an oxygen electrode (22). The abbreviations used are: NMDA, N-methyl-D-aspartate; ND, not detectable.

	DAAO						DASPO <sup>a</sup>		
	Wild-type			M213R			$k_{cat}$	$K_m$	$k_{cat}/K_m$
	$k_{cat}$	$K_m$	$k_{cat}/K_m$	$k_{cat}$	$K_m$	$k_{cat}/K_m$			
	$min^{-1}$	mM	$mM^{-1} min^{-1}$	$min^{-1}$	mM	$mM^{-1} min^{-1}$	$min^{-1}$	mM	$mM^{-1} min^{-1}$
D-Asp	29	18	1.6	235 (1665)	2 (28)	118 (58.5)	282	2.7	104
D-Glu	60	77.3	0.8	975	33	29.5	132	8.8	15
NMDA	ND	ND	ND	79	18	44	978	0.2	4890
D-Ala	5000	0.8	6100	630 (278)	17.8 (45.8)	35.4 (6.1)			
D-Pro	4640	21.5	216	1615	1280	1.3	24	0.9	27
D-Asn	1300	14.4	90	106	11	9.6			
D-Gln	1135	4.6	247	290	3.8	77			
D-Met	4600	0.2	25500	680	1.5	455			

<sup>a</sup> From Ref. 33.

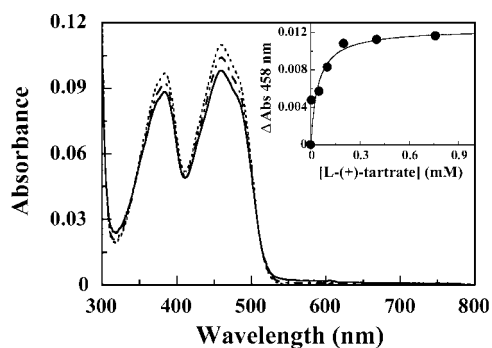


FIG. 3. Effect of L(+)-tartrate on the absorption spectrum of M213R RgDAAO. — indicates 8  $\mu$ M M213R DAAO in 50 mM HEPES, pH 7.5, 10% glycerol, 5 mM 2-mercaptoethanol, and 0.3 mM EDTA; after the addition of 0.05 mM (---) and 0.76 mM (····) (final concentration), respectively, of L(+)-tartrate in the same buffer as above. Inset, plot of the absorbance change at 458 nm as a function of L(+)-tartrate concentration.

TABLE III

Comparison of redox potentials of wild-type (26) and M213R mutant RgDAAO and of beef kidney DASPO (34).

$E_1$  is the oxidation-reduction potential for the couple  $EF1_{ox}/EF1_{seq}$ ;  $E_2$  is the potential for the couple  $EF1_{seq}/EF1_{red}$ ;  $E_m$  is the midpoint potential for the two-electron transfer (for the couple  $EF1_{ox}/EF1_{red}$ ). The redox potentials were measured at pH 7.5 and 15 °C using indigo tetrasulfonate (−43.3 mV), cresyl violet (−176 mV), and phenosafranine (−239 mV) as redox standards, and xanthine/xanthine oxidase as the source of reducing equivalents (25). The redox potentials of the complexed forms were measured in the presence of a saturating concentration of sodium benzoate (100 mM) for DAAO and of L(+)-tartrate (4 mM) for DASPO.

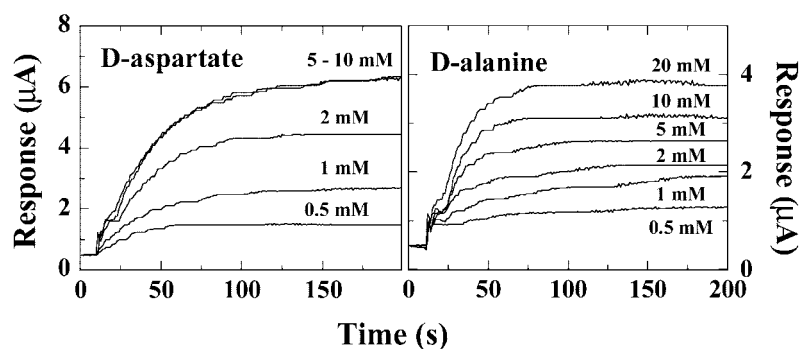
	DAAO		DASPO
	Wild-type	M213R	
Free form (mV)			
$E_1$	−50	−43	
$E_2$	−177	−177	
$E_m$	−106	−110	−96.5
Complexed form (mV)			
$E_1$	−116	−170	
$E_2$	−80	−217	
$E_m$	−98	−194	−156.5

DAAO under the same experimental conditions, the two-electron transfer was the thermodynamically favored process (maximum semiquinone was only ~20%) (26). To rigorously determine the potentials of the individual electron transfer, experiments were performed as detailed above in the presence of 100 mM sodium benzoate using cresyl violet and phenosafranine. Benzoate binding shifted the potentials of M213R DAAO in such a way that both  $E_1$  and  $E_2$  single-electron potentials are

more negative than in the free form (Table III). Binding of benzoate did not alter significantly the  $E_m$  values of wild-type DAAO at pH 7.5 (26); however, it strongly modulated the  $E_m$  value of the M213R mutant (see Table III). A similar change in the midpoint potential was observed for DASPO in the presence of L(+)-tartrate (35); even in the modulation of the redox properties by ligands, the M213R DAAO mutant resembled DASPO. The ~100 mV more negative  $E_m$  value of the DAAO-benzoate complex determined for the M213R mutant with respect to the wild-type DAAO could affect catalysis, because the more negative midpoint potential made enzyme reduction by D-alanine (rate-limiting for wild-type enzyme) slightly less thermodynamically favorable. The difference in redox potentials between M213R and wild-type DAAOs could point to a change in the FAD microenvironment (which fine tunes the enzyme reactivity) following the introduction of an additional basic group in the active site and which would be more evident in the complexed form of the enzyme. For this reason, the  $pK_a$  value for the deprotonation of the flavin N(3)H position was determined following the pH dependence of the visible spectrum of oxidized M213R DAAO. The value determined (Table I) did not show a significant change in comparison with the wild-type DAAO, indicating that the mutation did not affect the deprotonation of the N(3)H-flavin position.

**Purification and Properties of M213R/Y238R DAAO**—A low level of expression of the M213R/Y238R mutant was obtained in the BL21(DE3)pLysS *E. coli* cells using the protocol reported above for wild-type and M213R DAAO. The low expression of the double mutant was essentially due to inclusion bodies formation because Western blot analysis showed that the protein was present in the whole cell paste, but it was almost absent in the crude extracts. Nevertheless, a higher amount of mutant DAAO in the soluble fraction was not obtained by growing the cells at lower temperatures (25 and 30 °C), as well as inducing the DAAO synthesis at different  $A_{600}$ . Analogously, growing the cells without isopropyl-1-thio- $\beta$ -D-galactopyranoside addition up to 24–48 h and at different temperatures did not increase the amount of soluble DAAO mutant in the crude extract. Starting from a 1.5-liter fermentation broth (corresponding to 6 units of DAAO activity on D-alanine as substrate), 1.5 mg of pure enzyme with a specific activity of 0.46 units/mg protein was achieved. Like the wild-type enzyme, the purified variant DAAO was a dimeric holoenzyme, and the mutant enzyme was stable when stored at −20 °C, but it could not be used at 4 °C for more than 1 day, e.g. more than 80% of the protein was lost during overnight analysis. The visible spectrum of the oxidized form of the M213R/Y238R mutant enzyme showed the presence of the flavin peaks at ~452 and ~370 nm. Because of the low stability, only a limited kinetic

FIG. 4. Amperometric traces of D-aspartate (left) and D-alanine (right) detection using the M213R D-amino acid oxidase biosensor in the 0.5–20 mM substrate concentration range. Conditions: 0.17 units of M213R DAAO in 50 mM HEPES buffer, 10% glycerol, pH 7.5. Small volumes (25–250  $\mu$ l) of D-amino acid solution were added in the voltammetric cell (final volume of 5 ml in sodium pyrophosphate buffer, pH 8.5) while stirring and applying a fixed voltage (+400 mV versus Ag/AgCl).



characterization of this mutant DAAO was performed. The kinetic parameters of M213R/Y238R DAAO, determined at fixed (0.253 mM)  $O_2$  concentration using D-alanine and D-aspartate as substrates, are reported in Table II. The  $k_{cat}$  value of the double mutant on D-aspartate as substrate was 7-fold higher than that determined for the single (M213R) mutant, whereas the catalytic efficiency (expressed as  $k_{cat}/K_m$  ratio) on D-aspartate and D-alanine was decreased. Such a change was due to an increase in the  $K_m$  value for the substrate following the introduction of the second additional arginine in the active site of DAAO by site-directed mutagenesis. Such a negative contribution to substrate recognition and binding was also substantiated measuring the dissociation constant for L(+)-tartrate. Following the perturbation of the visible spectrum of the enzyme upon formation of the DAAO-ligand complex, a decrease in the binding of L(+)-tartrate was evident ( $K_d = 0.35$  mM).

**Amperometric Biosensor**—As an example of the practical applications, a DAAO biosensor for the determination of the D-amino acid concentration in food samples was developed starting from a commercial apparatus; the scheme of the flow in the electrochemical cell with RgDAAO adsorbed on the graphite electrode has been reported previously (20). As for the wild-type DAAO, a current in the system was recorded after adding 0.17 units of M213R mutant DAAO in the reaction chamber containing a D-alanine solution (at an applied potential of +400 mV). The current intensity increased with time, yielding a constant slope in the linear part of the curve within 2–3 min (Fig. 4). The slope, as well as the final value reached, depended on the D-alanine concentration (20). With wild-type DAAO no current was measured using D-aspartic acid as substrate. In contrast, the M213R enzyme can efficiently oxidize the D-amino acids with an acidic side chain, and thus a current response was obtained for these compounds (Fig. 4). Interestingly, the apparent  $K_m$  values determined for D-aspartate and D-alanine from primary and double-reciprocal plots of the current response at different substrate concentrations were in good agreement with the value determined for the free enzyme using the polarographic assay ( $K_m = 1.5 \pm 0.4$  versus  $2.0 \pm 0.4$  mM with D-aspartate and  $10.1 \pm 3.2$  versus  $17.8 \pm 7.7$  mM with D-alanine as substrate, respectively).

#### DISCUSSION

Rational design has been used to engineer the substrate specificity of DAAO, a flavoenzyme that is used in a variety of biotechnological applications (3). The three-dimensional structure of RgDAAO (7), in combination with site-directed mutagenesis studies (8–10), substantiated the role of the active site residues in substrate binding. In particular, the structure of RgDAAO in complex with D-alanine or trifluoro-D-alanine revealed the mode of substrate binding (Fig. 1A). By using the AutoDock program, a model of RgDAAO-D-aspartate complex was constructed. Since the three-dimensional structure of DASPO is unknown, we obtained a model of the DASPO-active

site based on the sequence homology between DAAO and DASPO. From a comparison of these active sites, we proposed that the residue located at the position of Met-213 in wild-type DAAO might play an important role in selecting the substrate specificity of DAAO. This hypothesis was further substantiated by docking D-aspartate at the active site of the M213R RgDAAO mutant (Fig. 2B), which showed an electrostatic interaction of the carboxylic side chain of the substrate with the side chain of Arg-213 and a correct orientation of the substrate with respect to the flavin redox site. To render the DAAO-active site more similar to the active site of the DASPO model, even the Tyr-238 was substituted with an arginine (Fig. 2C).

The mutation of Met-213 in arginine does not result in gross perturbation of FAD; thus the changes we observed were due to only specific and local structural modifications. On the other hand, the expressed double mutant DAAO remained insoluble, and the purified preparation also showed a low stability in solution, precluding a full characterization of its properties. The substrate specificity of the M213R mutant overlapped with that of DAAO and DASPO; it was still able to oxidize D-alanine and in the meantime the kinetic parameters on D-aspartate resemble that reported for DASPO (see Table II). The M213R mutant DAAO we produced represents a catalytic activity with a new, broader substrate specificity (not found in nature), because it was able to oxidize both neutral and acidic D-amino acids. On the other hand, the simultaneous presence of two additional arginines in the active site of DAAO (M213R/Y238R mutant) did not further increase the oxidative power of the enzyme on acidic D-amino acids but resulted in a decrease of the catalytic efficiency with both D-alanine and D-aspartate as substrate (Table II). This result could be ascribed to two different reasons as follows: (a) introduction of Arg-213 was adequate to render the DAAO-active site similar to that of DASPO; (b) the second arginine at position 238 was not significantly involved in substrate recognition. In fact the side chain of the Tyr-238 in DAAO was recently demonstrated to swing between two different conformations, the one observed in the DAAO-D-alanine complex (closed form) and that determined in the DAAO-anthranilate complex (open form) (Protein Data Bank code 1c0i). Results from site-directed mutagenesis experiments also support the conclusion that Tyr-238 played an important role controlling the product exchange at the active site, whereas it was only marginally involved in ligand/substrate selection and interaction (e.g. the  $K_d$  value for benzoate binding and the  $K_m$  value for D-alanine to Y238F mutant are 3–5-fold higher than the corresponding values determined for the wild-type DAAO) (10). Our results open the question concerning the role of Arg-237 in the active site of DASPO.

The effect of Met-213 substitution on RgDAAO kinetic properties can be explained in terms of the recently proposed mechanism in which “orbital steering/interactions are the predominant or the sole important factor in catalysis” (7, 13). The

perturbation of the active site in the M213R DAAO mutant modified the precise D-alanine alignment with respect to the N(5)-flavin position (alteration of the orbital trajectory resulted in a large decrease in the reaction velocity) and resulted in a large decrease in substrate affinity for neutral amino acids and in ligand binding for the classic carboxylic acids inhibitors (benzoate and anthranilate) of DAAO. On the other hand, this substitution allowed a better interaction with D-aspartate and D-glutamate. Furthermore, the presence of Arg-213 altered the redox properties of the flavin cofactor in the DAAO-benzoate complex, and thus, it also contributed to the decrease in the oxidative power. In fact, for L-lactate oxidase a linear dependence of the logarithm of the rate constants on the redox potential of enzyme reduction by L-lactate has been reported recently (36), employing reconstituted apoenzyme with a series of FMN analogs with different substituents at the 6- and 8- positions of the isoalloxazine ring, and thus with different redox potentials. In RgDAAO, an  $\approx 100$  mV more negative  $E_m$  value observed with the M213R mutant with respect to the wild-type in the benzoate complex form resulted in an  $\approx 35$ -fold decrease in maximal velocity with D-alanine as substrate. The additional arginine residue present at the active site of M213R mutant DAAO did not modify the distribution of charge surrounding the N(1)-C(2)=O flavin locus, as demonstrated by the observation that the  $pK_a$  value for the deprotonation of the N(3)H flavin position was unchanged. The modification of  $E_m$  as a function of benzoate presence could also result from very different values of the dissociation constants of benzoate binding to the oxidized and reduced M213R DAAO forms. A similar situation was recently reported (37) for the effect of pyruvate concentration on the apparent  $E_m$  value of R181M mutant of lactate oxidase. Because the  $K_d$  for pyruvate binding was 3 and 160 mM for the oxidized and the reduced lactate oxidase, respectively, the real redox midpoint was extrapolated at zero pyruvate concentration by plotting the apparent  $E_m$  value versus the pyruvate concentration. The determination of the constant binding for benzoate of reduced RgDAAO was not feasible. For the modulation of the redox properties by ligand binding, as well as for the turnover numbers and ligand-binding properties, the M213R DAAO mutant appeared to resemble DASPO.

In conclusion, we have shown that the substrate specificity of yeast DAAO was modulated by the amino acid side chains of the hydrophobic binding pocket of the active site that interacted with the side chain of the substrate. Among these residues, Met-213 appeared to be especially important. We thus have been successful in attaining a flavo-oxidase with a mutated and broader substrate specificity (which can be used to build up a biosensor for determining the entire content of D-amino acids in food specimens) using a structure-based rational protein design.

**Acknowledgment**—We thank Dr. Mauro Fasano for help with the ligand docking analyses.

## REFERENCES

- Massey, V., and Hemmerich, P. (1980) *Biochem. Soc. Trans.* **8**, 246–257
- Curti, B., Ronchi, S., and Pilone Simonetta, M. (1992) in *Chemistry and Biochemistry of Flavoenzymes* (Muller, F., ed) pp. 69–94, CRC Press, Inc., Boca Raton, FL
- Pilone, M. S. (2000) *Cell. Mol. Life Sci.* **57**, 1732–1747
- Pilone, M. S., Pollegioni, L., Casalin, P., Curti, B., and Ronchi, S. (1989) *Eur. J. Biochem.* **180**, 199–204
- Casalin, P., Pollegioni, L., Curti, B., and Pilone, M. S. (1991) *Eur. J. Biochem.* **197**, 513–517
- Pollegioni, L., Langkau, B., Fischer, W., Ghisla, S., and Pilone, M. S. (1993) *J. Biol. Chem.* **268**, 13850–13857
- Umhau, S., Pollegioni, L., Molla, G., Diederichs, K., Welte, W., Pilone, M. S., and Ghisla, S. (2000) *Proc. Natl. Acad. Sci. U. S. A.* **97**, 12463–12468
- Harris, C. M., Molla, G., Pilone, M. S., and Pollegioni, L. (1999) *J. Biol. Chem.* **274**, 36233–36240
- Molla, G., Porrini, D., Job, V., Motteran, L., Vegezzi, C., Campaner, S., Pilone, M. S., and Pollegioni, L. (2000) *J. Biol. Chem.* **275**, 24715–24721
- Pollegioni, L., Harris, C. M., Molla, G., Pilone, M. S., and Ghisla, S. (2001) *FEBS Lett.* **507**, 323–326
- Mattevi, A., Vanoni, M. A., Todone, F., Rizzi, M., Teplyakov, A., Coda, A., Bolognesi, M., and Curti, B. (1996) *Proc. Natl. Acad. Sci. U. S. A.* **93**, 7496–7501
- Pollegioni, L., Fukui, K., and Massey, V. (1994) *J. Biol. Chem.* **269**, 31666–31673
- Mesecar, A. D., Stoddard, B. L., and Koshland, D. E., Jr. (1997) *Science* **277**, 202–206
- Negri, A., Massey, V., and Williams, C. H. (1987) *J. Biol. Chem.* **262**, 10026–10034
- Burns, C. L., Main, D. E., Buckthal, D. J., and Hamilton, G. A. (1984) *Biochem. Biophys. Res. Commun.* **125**, 1039–1045
- Porter, D. J. T., Voet, J. G., and Bright, H. J. (1977) *J. Biol. Chem.* **252**, 4464–4473
- Negri, A., Massey, V., Williams, C. H., Jr., and Schopfer, L. M. (1988) *J. Biol. Chem.* **263**, 13557–13563
- Pilone, M. S., and Pollegioni, L. (2002) *Bioact. Biotrans.* **20**, 145–159
- Friedman, M. (1999) *J. Agric. Food Chem.* **47**, 3457–3479
- Sacchi, S., Pollegioni, L., Pilone, M. S., and Rossetti, C. (1998) *Biotechnol. Tech.* **12**, 149–153
- Sambrook, J., Fritsch, E. P., and Maniatis, T. (1989) *Molecular Cloning: A Laboratory Manual*, 2nd Ed., Cold Spring Harbor Laboratory Press, Cold Spring Harbor, NY
- Pollegioni, L., Falbo, A., and Pilone, M. S. (1992) *Biochim. Biophys. Acta* **1120**, 11–16
- Massey, V., and Hemmerich, P. (1978) *Biochemistry* **17**, 9–16
- Minnaert, K. (1965) *Biochim. Biophys. Acta* **110**, 42–56
- Massey, V. (1991) in *Flavins and Flavoproteins* (Curti, B., Ronchi, S., and Zanetti, G., eds) pp. 59–66, Walter de Gruyter & Co., Berlin
- Pollegioni, L., Porrini, D., Molla, G., and Pilone, M. S. (2000) *Eur. J. Biochem.* **267**, 6624–6632
- Guex, N., and Peitsch, M. C. (1997) *Electrophoresis* **18**, 2714–2723
- Faotto, L., Pollegioni, L., Cecilian, F., Ronchi, S., and Pilone, M. S. (1995) *Biotechnol. Lett.* **17**, 193–198
- Negri, A., Cecilian, F., Tedeschi, G., Simonic, T., and Ronchi, S. (1992) *J. Biol. Chem.* **267**, 11865–11871
- Goodsell, D. S., and Olson, D. J. (1990) *Proteins Struct. Funct. Genet.* **8**, 195–202
- Morris, G. M., Goodsell, D. S., Huey, R., and Olson, D. J. (1996) *J. Comput. Aided Mol. Des.* **10**, 293–304
- Molla, G., Vegezzi, C., Pilone, M. S., and Pollegioni, L. (1998) *Protein Expression Purif.* **14**, 289–294
- Tedeschi, G., Negri, A., Cecilian, F., Ronchi, S., Vetere, A., D'Aniello, G., and D'Aniello A. (1994) *Biochim. Biophys. Acta* **1207**, 217–222
- Clark, W. M. (1960) *Oxidation-Reduction Potentials of Organic Compounds*, pp. 184–203, Williams & Wilkins, Baltimore
- Negri, A., Tedeschi, G., Cecilian, F., and Ronchi, S. (1999) *Biochim. Biophys. Acta* **1431**, 212–222
- Yorita, K., Misaki, H., Palfey, B. A., and Massey, V. (2000) *Proc. Natl. Acad. Sci. U. S. A.* **97**, 2480–2485
- Yorita, K., Matsuoka, T., Misaki, H., and Massey, V. (2000) *Proc. Natl. Acad. Sci. U. S. A.* **97**, 13039–13044
- Pollegioni, L., Ghisla, S., and Pilone, M. S. (1992) *Biochem. J.* **286**, 389–394